

General Disclaimer

One or more of the Following Statements may affect this Document

- This document has been reproduced from the best copy furnished by the organizational source. It is being released in the interest of making available as much information as possible.
- This document may contain data, which exceeds the sheet parameters. It was furnished in this condition by the organizational source and is the best copy available.
- This document may contain tone-on-tone or color graphs, charts and/or pictures, which have been reproduced in black and white.
- This document is paginated as submitted by the original source.
- Portions of this document are not fully legible due to the historical nature of some of the material. However, it is the best reproduction available from the original submission.

REVISION OF GEODETIC PARAMETERS

E. M. Gaposchkin and M. R. Williamson

(NASA-CR-143331) REVISION OF GEODETIC
PARAMETERS (Smithsonian Astrophysical
Observatory) 26 p HC \$3.75 CSCL 08N

N75-30696

Unclassified
G3/46 33052

August 1975



Smithsonian Institution
Astrophysical Observatory
Cambridge, Massachusetts 02138



NG/CON-015-802

REVISION OF GEODETIC PARAMETERS

E. M. Gaposchkin and M. R. Williamson

ABSTRACT

Laser data from nine satellites and 12 stations are combined with surface-gravity data to obtain spherical harmonics representing the geopotential complete through degree and order 18. This laser-data-only solution provides a reasonable improvement to the gravity field.

INTRODUCTION

Smithsonian Astrophysical Observatory has published gravity-field solutions utilizing both satellite-tracking and terrestrial gravity data (see, e.g., Gaposchkin, 1974), which were based primarily on precision-reduced camera data and on then-available surface-gravity data. Now, however, we have better data, and new types of data will soon be available. The work reported here is the beginning of a general revision and extension of our knowledge of the geopotential. In this first iteration, we will experiment with new data (laser ranges), verify new methods of data reduction, and prepare for new types of data (altimeter and satellite-to-satellite tracking data). We seek here to improve our knowledge of the gravity field so that better satellite orbits, consistent with surface-gravity data, can be calculated. This is done by using laser data only, whose accuracy (approximately 1 m) is far greater than the ephemeris accuracy (approximately 10 m). The situation has changed since 1971, when the bulk of the data used were 4-arcsec camera data. Furthermore, substantial revisions have been made in the treatment of orbit perturbations, and all these

advances indicate a new attempt at improved geopotential coefficients.

OBJECTIVES

This computation has several objectives, the primary one being to use laser data only in a determination of the earth's gravity field, with the aim of computing satellite orbits to an accuracy comparable with that of the laser data. We can obtain a realistic gravity field consistent with surface-gravity data. A secondary objective is to study the consequences of using data that provide no ties to an inertial reference frame, as was the case with camera data. For our third objective, we will investigate the effects of one satellite on another in the solution; that is, we can optimize a solution for one satellite by using only data from that satellite. The question then becomes: How much does adding data from a second satellite degrade the orbit computed for the first? Of course, improved orbits and a more accurate geoid are necessary for analyzing satellite altimetry data for geodetic and oceanographic purposes.

REFINEMENTS AND TECHNIQUES

Improvements in perturbation calculations have been numerous. The inclination function for tesseral harmonics, as formulated by Kaula, computationally loses accuracy for high-degree coefficients. It has been replaced by a mathematically equivalent formula derived from group theory (Gaposchkin, 1973). The interaction terms between J_2 and resonant harmonics have also been improved. Lunar and solar perturbations and body tides and ocean tides have been computed to the necessary accuracy (Kozai, 1973). Perturbations arising from the noninertialness of the coordinate system have been corrected and improved (Kinoshita, 1975a,b),

and those due to direct solar radiation pressure (Aksnes, 1975), albedo pressure (Lautman, 1975a,b), and infrared radiation (Lautman, 1975c) have all been included and tested (Gaposchkin et al., 1975).

The compilation of surface-gravity data used in Gaposchkin (1974) has since been augmented (Williamson and Gaposchkin, 1975). The surface-gravity data are summarized in Table 1, and the distribution of these data is shown in Figure 1. Table 2 compares the $1^\circ \times 1^\circ$ gravity anomalies from the Defense Mapping Agency Aerospace Center (DMAAC, 1973) with other available compilations.

Three coordinated programs have provided laser tracking data in sufficient density to be used for a gravity-field determination: the International Satellite Geodesy Experiment (ISAGEX) held in 1971, the Earth Physics Satellite Observation Campaign (EPSOC) in 1972-1973, and the Geos 3 campaign in 1975. There has been a steady improvement in the volume, reliability, and accuracy of the data. One of the objectives of the ISAGEX program was to obtain data for determining the gravity field, and a number of orbital arcs are suitable for this purpose. The EPSOC program was directed to the study of long-period effects and polar motion. Some arcs from EPSOC are also used for determining the tesseral harmonics. Finally, during the current Geos 3 program routine data are being obtained and included in the analysis. Table 3 lists the participating stations for each campaign that are used in the analysis reported here. The distribution of the stations is shown in Figure 2.

Currently, nine satellites in orbit are equipped with cube-corner reflectors suitable for laser ranging; these satellites are useful for a gravity-field determination, especially as their distribution in inclination and height is reasonably good. Table 4 lists their orbital characteristics and the number of arcs used, and the distribution of satellites is given in Figure 3.

Satellite orbits are usually computed for between 8 and 16 days, the interval depending primarily on the availability of data. Also, each arc covers at least one oscillation of the resonant period. Table 5 gives the resonant periods for the satellites, while Table 6 lists the constants used to calculate the satellite orbits.

SOLUTIONS

The normal equations for surface-gravity data have been computed complete from degree 2 through 18. The combination solution included a number of harmonics of higher degree that are resonant with one or more of the satellite orbits. To this set of surface-gravity normal equations was added a set of normal equations, satellite by satellite. The system was solved after adding one satellite (Geos 1), and the result has been compared with all the satellites and with surface gravity. For the satellite comparison, one arc from each satellite was selected: generally, the arc with the most data. The orbit was recalculated with the revised gravity field, and the orbital fit in terms of σ_0 was used as the criterion. In all combinations, the satellite data were used at their a priori weight. The surface gravity was given several weights, and all solutions were tested in order to determine the optimum weight for the combination.

The weight finally adopted is

$$\langle A \rangle \frac{27}{nA} \text{ mgal} ,$$

where n is the number of $1^\circ \times 1^\circ$ squares in each $5^\circ \times 5^\circ$ mean, A is the area of the anomaly, and $\langle A \rangle$ is the average area. This weight is twice that used in the 1973 Smithsonian Standard Earth (III) (SE III) (Gaposchkin, 1973). The ISAGEX laser data were given a 5-m weight, and all other laser data, a 2-m weight.

These combination solutions are summarized in Tab' 7. The orbit for a satellite not used in the solution is really very poor, generally because of relatively small changes in a few coefficients resonant with the gravity field. We note that

Peole, which has no resonance, degrades marginally. The surface gravity $\langle(\Delta g_t - \Delta g_s)^2\rangle$ is only relative. A large part of those residuals is information in the higher harmonics. The best fit is obtained with only one satellite; however, when satellite data are added, the degradation is not large considering the overall accuracy of surface-gravity data.

Generally, adding satellite data also degrades the satellite orbit fit, but not very much. This overall improvement is considered quite satisfactory for one iteration of a very complex nonlinear process. All satellite orbits improved by at least 1 m^2 in the orbital fit. In percentage terms, Geos 1, BE-C, Geos 2, Starlette, Peole, and Geos 3 each improved in orbital fit by 17.9, 22.2, 43.9, 69.2, 26.2, and 13.6%, respectively, for an average 32% improvement!

The final adopted 52-arc solution (SE IV.1) can be compared with the surface-gravity data in more detail. Assuming they are statistically independent, the following quantities defined by Kaula (1966) can be computed and used to compare a geopotential model (g_s) with observed values of surface gravity (g_t):

$\langle g_t^2 \rangle$ The mean value of g_t^2 , where g_t is the mean free-air gravity anomaly based on surface gravity, indicating the amount of information contained in the surface-gravity anomalies.

$\langle g_s^2 \rangle$ The mean value of g_s^2 , where g_s is the mean free-air gravity anomaly computed from the geopotential model, indicating the amount of information in the computed gravity anomalies.

$\langle g_t g_s \rangle$ An estimate of g_h – i.e., the true value of the contribution to the gravity anomaly of the geopotential model and the amount of information common to both g_t and g_s .

$\langle (g_t - g_s)^2 \rangle$ The mean-square difference of g_t and g_s .

$E(\epsilon_s^2)$ The mean-square error in the geopotential model.

$E(\epsilon_t^2)$ The mean-square error of the observed gravity.

$E(\delta g^2)$ The mean square of the error of omission – that is, the difference between true gravity and g_h ; this term is then the model error.

If the geopotential model were perfect, then $\langle g_s^2 \rangle = \langle g_h^2 \rangle$, which in turn would equal $\langle g_t g_s \rangle$ if g_t were free from error and known everywhere. Then, ϵ_s^2 would be zero even though g_s would not contain all the information necessary to describe the total field. The information not contained in the model field — i.e., the error of omission, δg — then consists of the higher order coefficients. The quantity $\langle (g_t - g_s)^2 \rangle$ is a measure of the agreement between the two estimates g_t and g_s and is equal to

$$\langle (g_t - g_s)^2 \rangle = E(\epsilon_s^2) + E(\epsilon_t^2) + E(\delta g^2) .$$

Another estimate of g_h can be obtained from the gravimetric estimates of degree variance σ_ℓ^2 (Kaula, 1966):

$$E(g_h^2) = D = \sum_\ell \frac{n_\ell}{2\ell + 1} \sigma_\ell^2 ,$$

where n_ℓ is the number of coefficients of degree ℓ included in g_h , and

$$\sigma_\ell^2 = \gamma^2 (\ell - 1)^2 \sum_m \left(\bar{c}_{\ell m}^2 + \bar{s}_{\ell m}^2 \right) .$$

We also have

$$E(\epsilon_s^2) = \langle g_s^2 \rangle - \langle g_s g_t \rangle$$

and

$$E(\epsilon_t^2) = \langle g_t^2 \rangle / \langle n \rangle .$$

These values are given in Table 8 for SE III and for this solution.

The information in the surface-gravity data solution $\langle g_t^2 \rangle$ has increased in this new data set. This is reasonable; since the unobserved areas had an expected value of zero, the fewer observed areas there are, the lower the variance is. However, the information in the satellite solution $\langle g_s^2 \rangle$ has decreased, a fact that is confirmed by a decrease in D. Therefore, the information in SE III was too high. The residual $\langle (g_t - g_s)^2 \rangle$ has remained roughly the same, while the information in the higher harmonics is estimated to be larger. The estimate of $E(\epsilon_s^2)$ cannot be good, as these sets of data, g_s and g_t , are not independent.

The spherical-harmonic coefficients are listed in Tables 9 and 10. Figure 4 is a plot of the mean potential coefficient as a function of degree, and Figures 5 and 6 show the geoid height and gravity anomalies for this solution.

FUTURE WORK

The obvious next step is to complete another iteration, taking the solution to perhaps degree and order 24. To this can be added the normal equations for zonal harmonics and sets of resonant harmonics. When the orbital accuracy approaches a few meters, then we must reduce the error in the station coordinates by solving for them. Finally, of course, the aim is to add altimetry data to this system of normal equations.

In summary, we find that the improved accuracy that has been apparent from laser data is becoming realized.

ACKNOWLEDGMENT

This work was supported in part by grant NGR 09-015-002 from the National Aeronautics and Space Administration.

REFERENCES

ACIC, 1971. $1^\circ \times 1^\circ$ mean free-air gravity anomalies. Aeronautical Chart and Information Center Ref. Publ. No. 29, August, 324 pp.

Aksnes, K., 1975. Short-period and long-period perturbations of a spherical satellite due to direct solar radiation. *Celest. Mech.*, in press.

DMAAC, 1973. $1^\circ \times 1^\circ$ mean free-air gravity anomalies. Defense Mapping Agency Aerospace Center Ref. Publ. No. 73-0002, December, 100 pp.

Gaposchkin, E.M., editor, 1973. 1973 Smithsonian Standard Earth (III). Smithsonian Astrophys. Obs. Spec. Rep. No. 353, 388 pp.

Gaposchkin, E. M., 1974. Earth's gravity field to eighteenth degree and geocentric coordinates for 104 stations from satellite and terrestrial data. *Journ. Geophys. Res.*, vol. 79, pp. 5377-5411.

Gaposchkin, E. M., Latimer, J., and Mendes, G., 1975. Station coordinates in the Standard Earth III system and radiation-pressure perturbations from ISAGEX camera data. Presented at the International Association of Geodesy Meeting, Grenoble, France, August.

Kahle, H. G., and Talwani, M., 1973. Gravimetric Indian Ocean geoid. *Zs. f. Geophys.*, vol. 39, pp. 164-187.

Kaula, W. M., 1966. Tests and combinations of satellite determinations of the gravity fields with gravimetry. *Journ. Geophys. Res.*, vol. 71, pp. 5303-5314.

Kinoshita, H., 1975a. Formulas for precession. *Smithsonian Astrophys. Obs. Spec. Rep.*, in preparation.

Kinoshita, H., 1975b. Theory of the rotation of the rigid earth. *Smithsonian Astrophys. Obs. Spec. Rep.*, in preparation.

Kozai, Y. 1973. A new method to compute lunisolar perturbations in satellite motions. *Smithsonian Astrophys. Obs. Spec. Rep.* No. 349, 27 pp.

Lautman, D. A., 1975a. Perturbations of a close-earth satellite due to sunlight diffusely reflected from the earth. Submitted to *Celest. Mech.*

Lautman, D. A., 1975b. Perturbations of a close-earth satellite due to sunlight diffusely reflected from the earth. II. Variable albedo. To be submitted to *Celest. Mech.*

Lautman, D. A., 1975c. Perturbations of a close-earth satellite due to delayed infrared emission from the earth. *Celest. Mech.*, in preparation.

Mather, R., 1970. The Australian geodetic datum in earth space. *UNISURV Rep.* No. 19, Univ. New South Wales, p. 80.

Talwani, M., Poppe, H. R., and Rabinowitz, P. D., 1972. Gravimetrically determined geoid in the western North Atlantic. In Sea-Surface Topography from Space, vol. II, ed. by J. Apel, NOAA Tech. Rep. ERL 228-AOML 7-2, pp. 23-1 to 23-33.

Williamson, M. R., and Gaposchkin, E.M., 1975. The estimation of 550 km x 550 km mean gravity anomalies. *Smithsonian Astrophys. Obs. Spec. Rep.* No. 363, 21 pp.

Table 1. Surface-gravity data available.

Source	No. of $1^\circ \times 1^\circ$ means	No. of 550 x 550 km blocks $n \geq 1$	No. of 550 x 550 km blocks $n = 25$
Gaposchkin (1974)	19328	1183	145
Williamson and Gaposchkin (1975)	31636	1452	485
Maximum number	64800	1690	1690

Table 2. Comparison of $1^\circ \times 1^\circ$ mean gravity anomalies with DMAAC (1973).

Source	No. of points compared	Mean difference (mgal)	rms (mgal)
Australia (Mather, 1970)	1364	1.64	24.16
North America and North Atlantic (Talwani <i>et al.</i> , 1972)	3613	-0.18	15.29
Indian Ocean (Kahle and Talwani, 1973)	2226	-1.66	23.09
Worldwide (ACIC, 1971)	19164	-0.23	16.99

Table 3. Lasers stations used in this analysis.

Number	Station	Agency	ISAGEX	EPSOC	Geos 3
7902	Olifantsfontein, S. Africa	SAO	x	x	x
7907	Arequipa, Peru	SAO	x	x	x
7921	Mt. Hopkins, Arizona	SAO	x	x	x
7928	Natal, Brazil	SAO	x	x	x
7930	Athens, Greece	SAO	x		x
7050	GSFC	NASA	x		x
7060	Guam	NASA	x		
7061	San Diego, Calif.	NASA		x	
7080	Quincy, Calif.	NASA		x	
7068	Grand Turk Island	NASA			x
7804	San Fernando, Spain	CNES	x		
7809	Haute Provence, France	CNES	x		

Table 4. Summary of dynamical data.

Satellite Designation	Name	Inclination	Eccentricity	Perigee height (km)	a (km)	Number of arcs
7010901	Peole	15°	0.017	635	7070	5
6701401	D1D	39	0.053	569	7337	3
6701101	D1C	40	0.052	579	7336	2
6503201	BE-C	41	0.026	941	7311	9
7501001	Starlette	50	0.0207	805	7335	5
6508901	Geos 1	59	0.073	1121	8074	14
7502701	Geos 2	-65	0.0005	840	7222	4
6800201	Geos 3	-75	0.031	1101	7709	8
6406401	BE-B	80	0.012	912	7362	2
Total						52

Table 5. Resonant periods.

Satellite	Resonant with order m	Period (days)
7010901	none	
6701401	13	9.4
6701101	14	2.6
6503201	13	5.6
7501001	14	3.2
6508901	12	7.2
7502701	14	3.9
6800201	13	6.3
6406401	14	2.9

Table 6. Constants used in orbit computation.

GM = 3.986013×10^{20} cm ³ sec ⁻²	
c = 2.997925×10^{10} cm sec ⁻¹ = speed of light	
$k_2 = 0.25$ = Love's number	
$\epsilon_2 = 10^\circ$ = phase lag of tide	
$a_e = 6.378140$ Mm	
$\alpha = 0.32$ = earth's albedo	
Satellite	
	A/m (cm ² g ⁻¹)
7010901	0.20
6701401	0.30
6701101	0.30
6503201	0.13
7501001	0.01
6508901	0.10
7502701	0.04
6800201	0.06
6406401	0.10

Table 7. Comparison of solutions.

Solution	No. of arcs	$\langle (\Delta g_t - \Delta g_s)^2 \rangle, \text{gal}^2$	Surface gravity			Geos 1	BE-C	Geos 2	Starlette	People	Geos 3				
			n ≥ 1	n ≥ 20	σ_0	n	σ_0	n	σ_0	n	σ_0				
SE III	(203)	193	135	4.53	3021	5.81	1699	5.58	1112	16.61	2443	15.41	805	13.16	1076
Geos 1	(5)	123	86	3.15	3033	38.87	1688	32.60	1126	24.14	2336	16.16	797		
and BE-C	(5)	130	89	3.12	3004	4.22	1701	133	1140	770	2344	12.35	796		
and Geos 2	(5)	132	91	3.38	3012	4.20	1689	3.23	1125	18.11	2316	12.59	794		
Geos 1	(14)														
BE-C	(9)														
Geos 2	(8)														
BE-B	(2)														
DID	(3)														
DIC	(2)														
People	(5)														
Starlette	(5)														
and Geos 3	(4)	142	100	3.72	3022	4.52	1695	3.13	1122	5.12	2258	11.38	794	11.37	1075

ORIGINAL PAGE IS
OF POOR QUALITY

Table 8. Comparison of surface gravity with solution ($\text{mga}1^2$); all solutions are to the 18th degree and order.

Solution	$\langle (g_t - g_s)^2 \rangle$	$\langle g_t g_s \rangle$	$\langle g_s^2 \rangle$	D	$\langle g_t^2 \rangle$	$E(\epsilon_s^2)$	$E(\epsilon_t^2)$	$E(\delta_g^2)$	n*
SE III+	156	202	258	237	302	56	24	75	$n \geq 1$ (1183)
SE III+	117	255	281	237	345	26	19	63	$n \geq 10$ (659)
SE III+	105	221	236	237	311	15	13	77	$n \geq 20$ (301)
SE III	135	237	254	235	356	16	15	104	$n \geq 20$ (678)
SE IV.1	142	192	217	227	309	25	19	98	$n \geq 1$ (1452)
SE IV.1	103	232	235	227	333	2	16	85	$n \geq 10$ (1056)
SE IV.1	100	250	244	227	356	-6	15	92	$n \geq 20$ (678)

* n is the number of $1^\circ \times 1^\circ$ mean gravity anomalies in the $5^\circ \times 5^\circ$ mean gravity anomalies.

+ From the available data, there were 1183, 659, and 306 gravity anomalies with $n = 1, 10$, and $20 1^\circ \times 1^\circ$ anomalies.

Table 9. SE IV.1 fully normalized tesseral-harmonic coefficients for the geopotential (in units of 10^{-6}).

ORIGINAL PAGE IS
OF POOR QUALITY

Table 10. SE III fully normalized zonal harmonic coefficients for the geopotential (in units of 10^{-6}).

L	M	C
2	0	-484.16999
6	0	-15310
10	0	-05172
14	0	-01950
18	0	-01677
22	0	-01371

FIGURE CAPTIONS

Figure 1. Distribution of $1^{\circ} \times 1^{\circ}$ mean surface-gravity data.

Figure 2. Locations of the observing stations included in SE IV.1.

Figure 3. Distribution of perigee heights and inclinations of the satellites used in SE IV.1.

Figure 4. Mean potential coefficient by degree.

Figure 5. SE IV.1 geoid height in meters calculated with respect to the best-fitting ellipsoid, $f = 1/298.256$.

Figure 6. SE IV.1 gravity anomalies in milligals calculated with respect to the best-fitting ellipsoid, $f = 1/298.256$.

PRECEDING PAGE BLANK NOT FILMED



Figure 1. Distribution of $1^\circ \times 1^\circ$ mean surface-gravity data.

ORIGINAL PAGE IS
OF POOR QUALITY

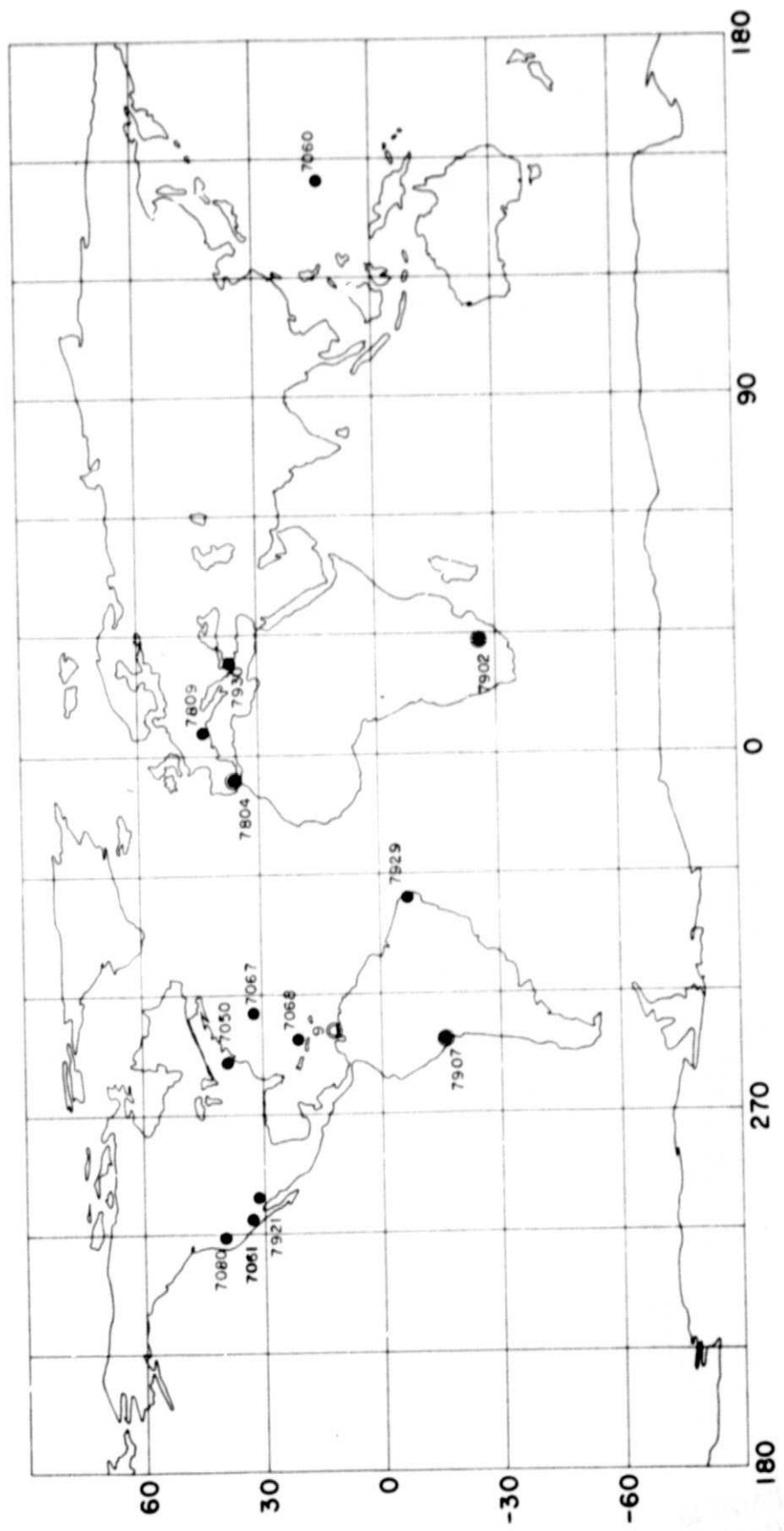


Figure 2. Locations of the observing stations included in SE IV.1.

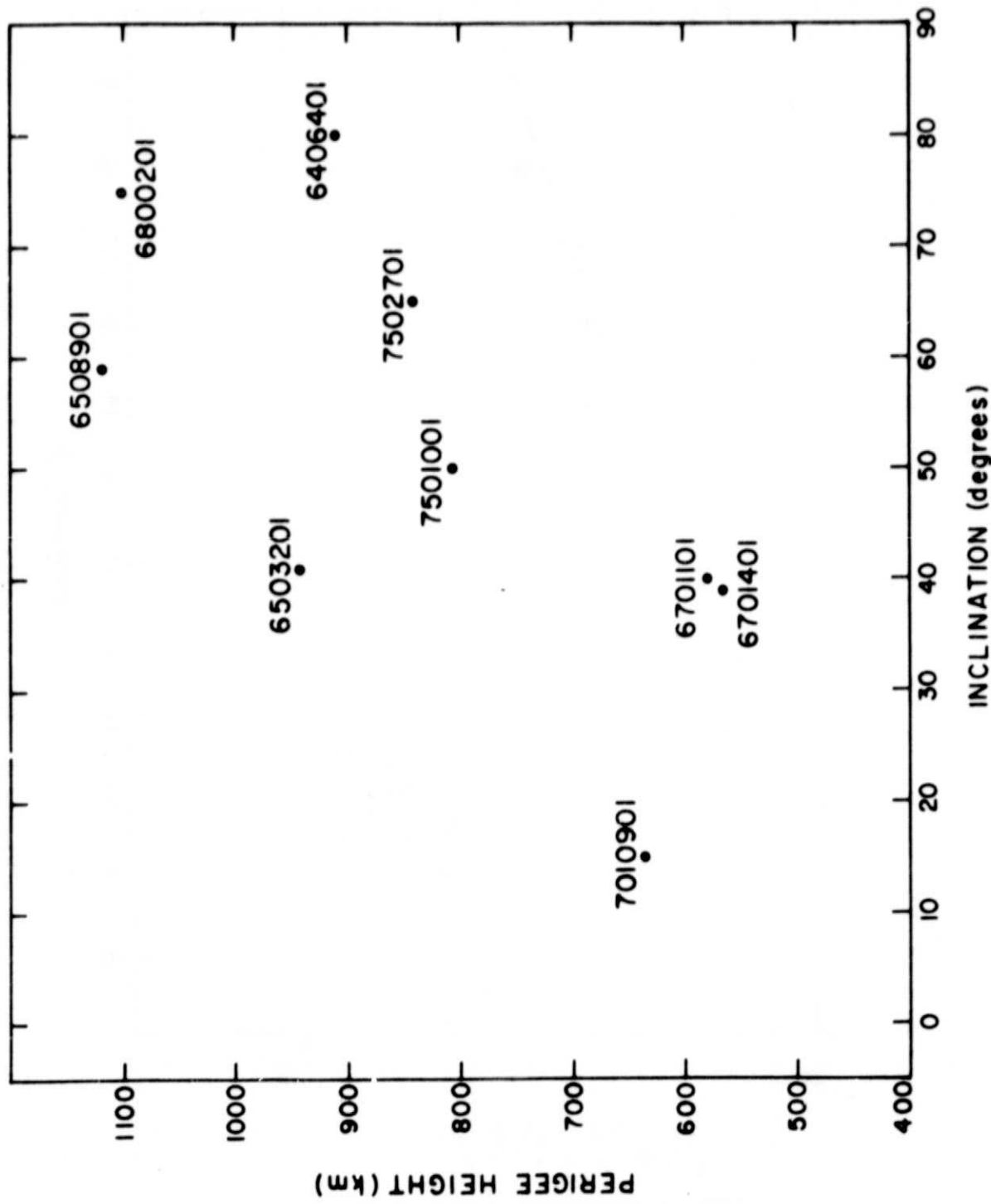


Figure 3. Distribution of perigee heights and inclinations of the satellites used in SE IV.1.

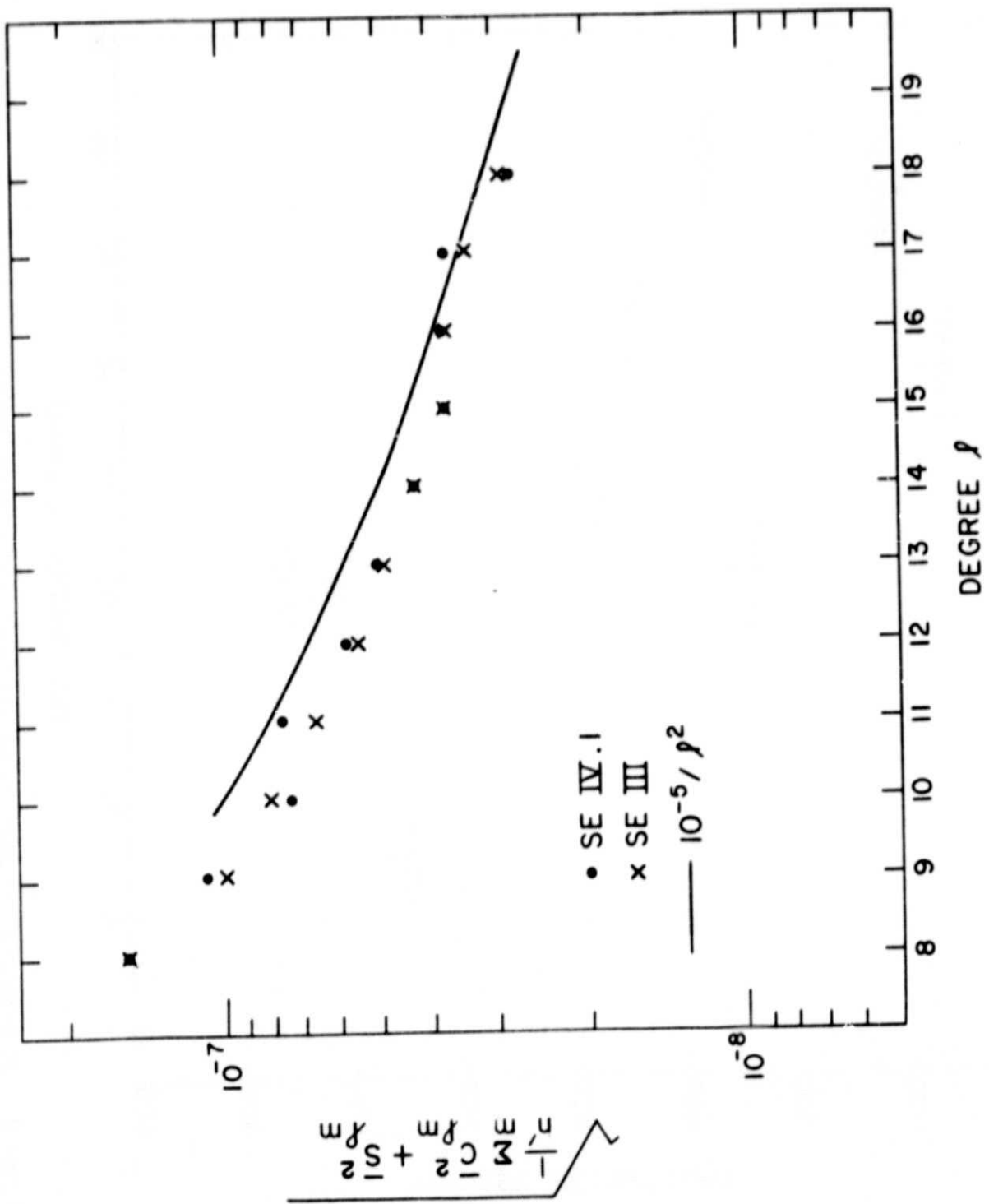


Figure 4. Mean potential coefficient by degree.

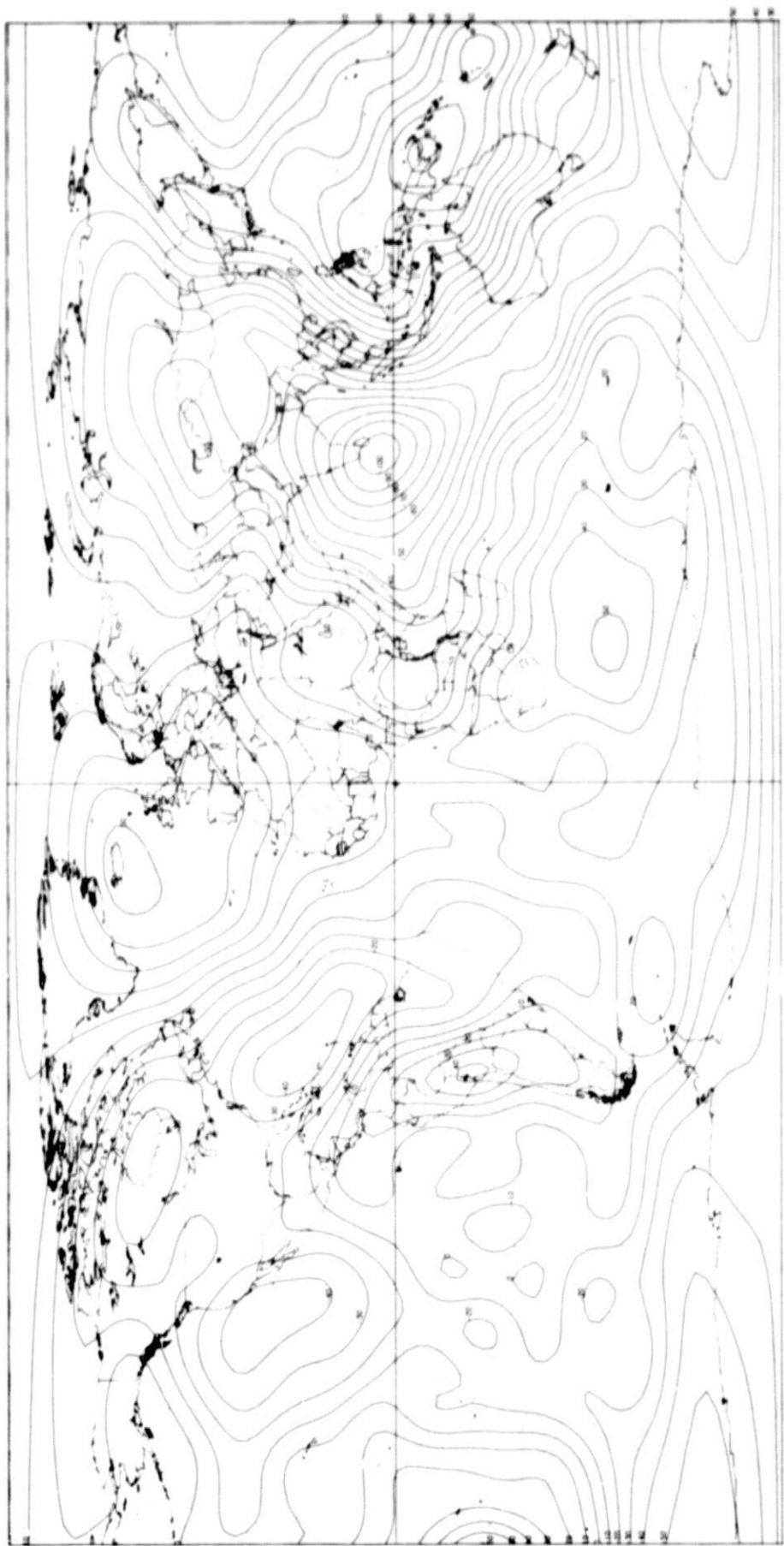


Figure 5. SE IV.1 geoid height in meters calculated with respect to the best-fitting ellipsoid, $f = 1/298.256$

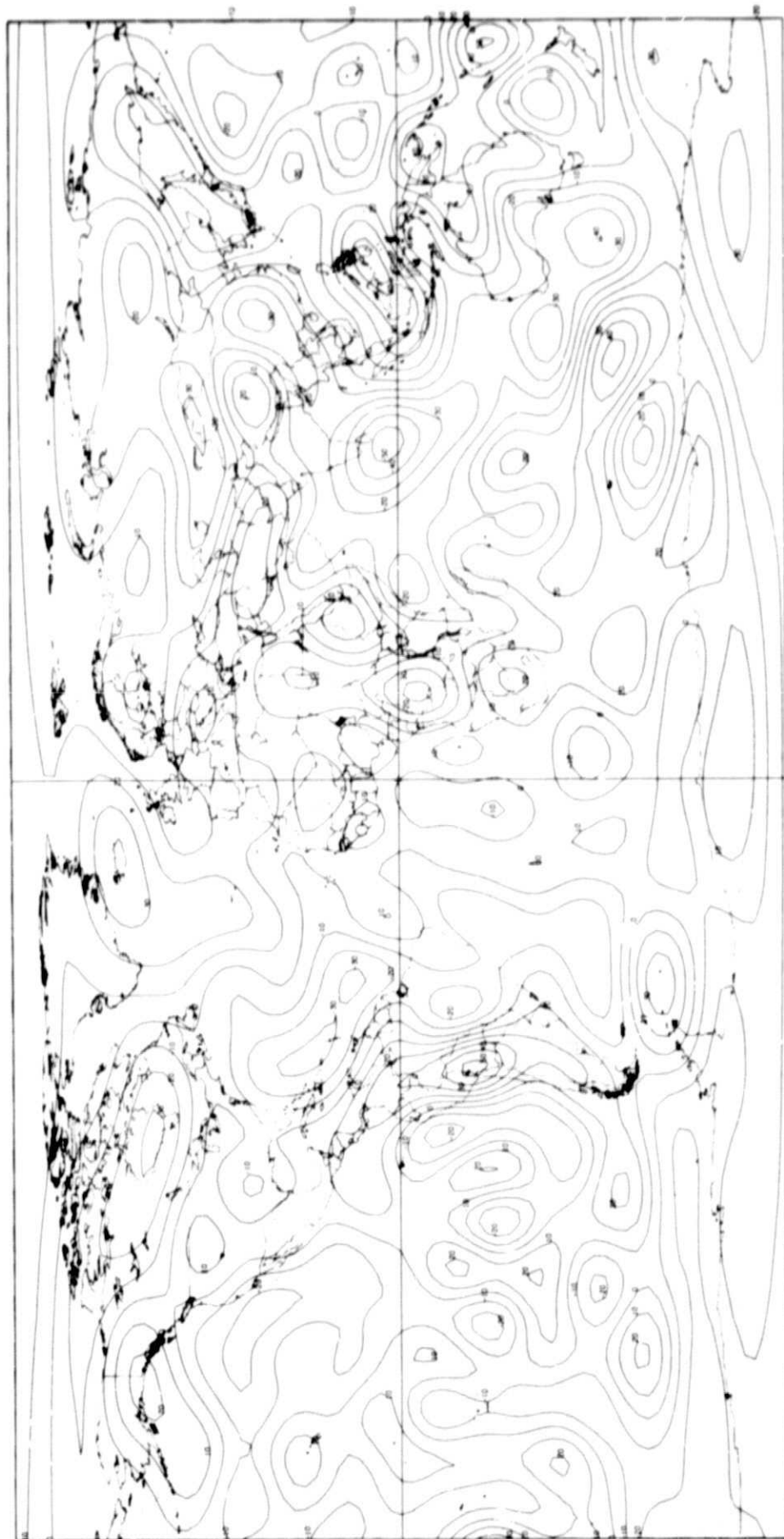


Figure 6. SE IV.1 gravity anomalies in milligals calculated with respect to the best-fitting ellipsoid, $f = 1/298.256$